HHS Public Access

Author manuscript

Oncogene. Author manuscript; available in PMC 2014 January 18.

Published in final edited form as:

Oncogene. 2013 July 18; 32(29): 3420–3431. doi:10.1038/onc.2012.355.

Mer or Axl Receptor Tyrosine Kinase Inhibition Promotes Apoptosis, Blocks Growth, and Enhances Chemosensitivity of Human Non-Small Cell Lung Cancer

Rachel M.A. Linger, PhD[1], **Rebecca A. Cohen, BS**[1], **Christopher T. Cummings, BS**[1], **Susan Sather, BS**[1], **Justine Migdall-Wilson, BA**[1], **Deryck H.G. Middleton, BS**[2], **Xian Lu, MS**[3], **Anna E. Barón, PhD**[3], **Wilbur A. Franklin, MD**[4], **Daniel T. Merrick, MD**[4,6], **Paul Jedlicka, MD, PhD**[4], **Deborah DeRyckere, PhD**[1], **Lynn E. Heasley, PhD**[5], and **Douglas K. Graham, MD, PhD**[1]

[1]Department of Pediatrics, Section of Hematology, Oncology, and Bone Marrow Transplantation, University of Colorado Anschutz Medical Campus, Aurora, CO 80045 USA

[2]Program in Cancer Biology, University of Colorado Anschutz Medical Campus, Aurora, CO 80045 USA

[3]Department of Biostatistics and Informatics, University of Colorado Anschutz Medical Campus, Aurora, CO 80045 USA

[4]Department of Pathology, University of Colorado Anschutz Medical Campus, Aurora, CO 80045 USA

[5]Department of Craniofacial Biology, University of Colorado Anschutz Medical Campus, Aurora, CO 80045 USA

[6]Department of Pathology, Denver VA Medical Center, Denver, CO 80220 USA

Abstract

Non-small cell lung cancer (NSCLC) is a prevalent and devastating disease that claims more lives than breast, prostate, colon, and pancreatic cancers combined. Current research suggests that standard chemotherapy regimens have been optimized to maximal efficiency. Promising new treatment strategies involve novel agents targeting molecular aberrations present in subsets of NSCLC. We evaluated 88 human NSCLC tumors of diverse histology and identified Mer and Axl as receptor tyrosine kinases (RTKs) overexpressed in 69% and 93%, respectively, of tumors relative to surrounding normal lung tissue. Mer and Axl were also frequently overexpressed and activated in NSCLC cell lines. Ligand-dependent Mer or Axl activation stimulated MAPK, AKT, and FAK signaling pathways indicating roles for these RTKs in multiple oncogenic processes. In addition, we identified a novel pro-survival pathway—involving AKT, CREB, Bcl-xL, survivin,

Corresponding Author: Douglas K. Graham, MD, PhD; Department of Pediatrics, Mail Stop 8302, 12800 East 19th Avenue, Aurora, CO 80045 USA; doug.graham@ucdenver.edu; phone 303-724-4006; fax 303-724-4015.

Conflict of Interest Statement

The authors declare no conflicts of interest.

Supplementary Information

Supplementary Information is available at *Oncogene's* website.

and Bcl-2—downstream of Mer, which is differentially modulated by Axl signaling. We demonstrated that shRNA knockdown of Mer or Axl significantly reduced NSCLC colony formation and growth of subcutaneous xenografts in nude mice. Mer or Axl knockdown also improved in vitro NSCLC sensitivity to chemotherapeutic agents by promoting apoptosis. When comparing the effects of Mer and Axl knockdown, Mer inhibition exhibited more complete blockade of tumor growth while Axl knockdown more robustly improved chemosensitivity. These results indicate that Mer and Axl play complementary and overlapping roles in NSCLC and suggest that treatment strategies targeting both RTKs may be more effective than singly-targeted agents. Our findings validate Mer and Axl as potential therapeutic targets in NSCLC and provide justification for development of novel therapeutic compounds that selectively inhibit Mer and/or Axl.

Keywords

targeted therapy; receptor tyrosine kinase; MerTK; signal transduction; xenograft; chemosensitivity

Introduction

Lung cancer is the primary cause of cancer-related death worldwide. Although prostate and breast cancer are the most frequently diagnosed cancers in men and women, respectively, lung cancer kills more people than prostate, breast, colon, and pancreatic cancers combined [1]. The current 5-year survival rate for all stages of non-small cell lung cancer (NSCLC) combined is 17% [2]. Significant focus on targeted therapeutics has resulted in approval of new drugs for lung cancer, including inhibitors of the epidermal growth factor receptor (EGFR) and anaplastic lymphoma kinase (ALK). These agents have improved outcome in approximately 10% and 5% of NSCLC cases, respectively, where *EGFR* mutation or *ALK* rearrangements are present [3, 4]. Mutations in *KRAS* (10–20%), *PI3KCA* (3%), *BRAF* (3%), and *ERBB2* (2%) have been found in additional subsets of NSCLC [5–8]. Preclinical target validation studies have demonstrated the utility of inhibiting these mutant proteins and numerous agents are currently in various phases of clinical development for use in lung cancer [9–14]. The remaining majority of NSCLC diagnoses represent an unmet need for identification of oncogenic drivers—and novel therapeutic targets—in these molecularly undefined cases. To address this problem, we have investigated the roles of Mer and Axl receptor tyrosine kinases (RTKs) as novel oncogenic molecules in lung cancer.

Mer and Axl are members of the TAM family of RTKs [15]. TAM receptors have been implicated in the development and metastasis of many cancers, including hematologic malignancies and solid tumors of the brain and breast [16, 17]. Previous studies identified Axl as a potential therapeutic target in NSCLC [18, 19], particularly in adenocarcinoma, where Axl expression correlated with advanced disease stage [20]. A proteomic study ranked both Mer and Axl among the top 20 most phosphorylated RTKs in a subset of NSCLC tumors [21], but there are no other published reports investigating the role of Mer in NSCLC. This paper identifies Mer and Axl as frequently overexpressed and activated RTKs in human NSCLC,

and proposes a mechanism by which Mer and/or Axl inhibitors may improve the efficacy of current NSCLC chemotherapy regimens.

Results

Mer and Axl are frequently overexpressed and activated in NSCLC

We evaluated expression of Mer and Axl RTKs in 88 NSCLC patients. Demographic and histopathologic data are presented in Table 1. Consistent with previous reports, survival was associated with stage of disease, but not histology [2, 22]. Tumor cells exhibited membranous and cytoplasmic staining for Mer and Axl (Fig. 1A and Supplemental Fig. 1A). Mer expression was detected (H-Score ≥ 5) in 69% of patients (Table 1) and was generally low to moderate with a median H-Score of 15 (range: 0–213). However, intermediate (H-Score = 101–300) Mer expression was observed in 5% of patients. Axl expression was detected in 93% of patients and tended to be higher than Mer (median H-Score: 175, range: 0–375) with intermediate and high (H-Score ≥ 301) expression observed in 66% and 6% of patients, respectively. Normal lung tissue adjacent to tumors was always negative for Mer and Axl, as was bronchial epithelium (Fig. 1A and Supplemental Fig. 1A), indicating upregulated expression of both Mer and Axl specifically in cancer cells. Within the tumor microenvironment, Mer was strongly expressed in cells exhibiting macrophage morphology, while Axl expression intensity was variable. Axl, but not Mer, was strongly expressed in blood vessels (Fig. 1A and Supplemental Fig. 1A and 1B). Mer expression did not correlate with Axl expression, suggesting that these related RTKs may have different roles in the pathogenesis of NSCLC. Mer and Axl expression were not associated with overall patient survival and did not differ significantly by stage or histology (Table 1 and data not shown).

Mer and Axl were also frequently overexpressed in a panel of NSCLC cell lines relative to normal human bronchial epithelial (NHBE) cells. In general, Mer and Axl protein expression patterns (Fig. 1B) were consistent with mRNA levels (Fig. 1C). Mer protein was overexpressed in 12/13 NSCLC cell lines relative to NHBE cells where Mer was undetectable. Expression of Mer mRNA was significantly higher in 9/13 NSCLC cell lines (0.03 – 2.3, $P < 0.01$) relative to NHBE cells (0.004). Axl protein was overexpressed in 9/13 NSCLC cell lines relative to the low level present in NHBE cells. Axl mRNA levels were higher in H1299, H157, HCC15, and H2009 cells (0.68–2.35) relative to NHBE cells (0.36). Significantly lower levels of Axl mRNA were found in the H358 (0.13, $P < 0.001$) and H1648 (0.03, $P < 0.001$) cells relative to NHBE and Axl mRNA was undetectable in Colo699 cells. Mer and Axl were highly phosphorylated under normal culture conditions in several NSCLC cell lines (Fig. 1D). Relative Mer phosphorylation (pMer/total Mer) was highest in Colo699, H1299, and A549 cells, while relative Axl phosphorylation was highest in H2009, H1299, and A549 cells. These data are consistent with a proteomic study that identified Axl and Mer as highly phosphorylated in NSCLC tumors and cell lines [21].

Mer and Axl activate multiple oncogenic signaling modules

Activation of Mer and Axl stimulates proliferative and anti-apoptotic signaling, including the PI3K/AKT and MAPK/ERK pathways [15]. We utilized a phospho-kinase array to investigate whether these and/or other oncogenic signaling pathways were activated

downstream of Mer in NSCLC cells. Colo699 cells were used for this experiment because they express high levels of Mer and do not express Axl (Fig. 1B), thereby eliminating complications due to Axl activation by the shared ligand Gas6 (Fig. 2A). Nine proteins (p38α, ERK1/2, GSK3α/β, MEK1/2, MSK1/2, AKT, mTOR, CREB, and FAK) exhibited increased phosphorylation following Gas6 treatment (Figs. 2B and 2C). We verified our findings in Colo699 cells as well as three additional NSCLC cell lines (A549, H2009, and HCC15) by immunoblotting (Fig. 2D). The most robust responses to Gas6 stimulation—which could be observed in all four cell lines—were phosphorylation of FAK, AKT, GSK3α/β, and ERK1/2. Gas6-induced CREB phosphorylation was most notable in H2009 cells. An additional protein, ATF1, was identified as Gas6-responsive in H2009 and Colo699 cells due to cross-reactivity of the anti-phospho-CREB antibody with phospho-ATF1. ATF1, a CREB family transcription factor, is activated downstream of MSK1/2 in response to both growth factors and cellular stress [23]. The ten proteins most highly phosphorylated in response to Gas6 indicate activation of MAPK (MEK1/2, ERK 1/2, p38α, MSK1/2, CREB, and ATF1), AKT (AKT, GSK3, and mTOR), and FAK signaling modules downstream of Mer in NSCLC cells (Fig. 2E). Since Axl is expressed and activated by Gas6 in the A549, H2009, and HCC15 cell lines, we cannot rule out contributions of Axl to these signaling pathways. These data suggest roles for Mer and/or Axl in multiple oncogenic processes including cell growth, proliferation, survival, and migration.

RNAi depletion of Mer or Axl predisposes NSCLC cells to apoptosis and inhibits pro-survival signaling

To assess the functional consequences of blocking anti-apoptotic Mer and Axl signaling pathways, we utilized a short-term YO-PRO-1/PI assay. A549 cells were used for these studies because they exhibit high relative phosphorylation of both Mer and Axl under normal culture conditions (Fig. 1D). Constitutive knockdown of Axl (shAxl8, shAxl9) or Mer (shMer1, shMer4) was achieved in polyclonal A549 populations transduced with two different target-specific shRNA sequences (Fig. 3A). Clonal isolates were generated from the shAxl8, shAxl9, and shMer1 populations (shAxl8-G5, shAxl9-D3, and shMer1-G8, respectively). In general, clonal populations exhibited more robust knockdown of Mer or Axl than polyclonal populations. Under basal culture conditions, a significant fraction of shMer1 cells exhibited increased staining with YO-PRO-1 relative to shControl cells, indicating a higher rate of apoptosis (Fig. 3B). Upon serum starvation, increased YO-PRO-1 staining in shMer1 cells was accompanied by increased PI uptake, indicating an accumulation of both apoptotic and dead cells. Mer-knockdown A549 cells exhibited higher rates of basal (37%, $P < 0.01$) and serum withdrawal-induced (52%, $P < 0.01$) apoptosis relative to shControl cells (5% and 20%, respectively) (Fig. 3C). Evaluation of shAxl8 A549 cells revealed a non-significant trend towards more cell death under both basal (14%, $P > 0.05$) and serum-free (33%, $P > 0.05$) conditions relative to shControl cells. NSCLC cells are known to overexpress the pro-survival proteins Bcl-2 and Bcl-xL [24, 25], which are transcriptionally activated by the AKT/CREB signaling pathway [26] identified as downstream of Mer activation in Figure 2. Activation of these and other pro-survival signaling proteins was evaluated by western blotting of A549 whole-cell lysates following serum starvation for two hours to replicate the experimental conditions applied in Figures 3B and 3C. Relative to control A549 cells (wild type and shControl), Mer-knockdown A549

cells (shMer1-G8) exhibited a dramatic reduction in phosphorylation of AKT that correlated with reduced expression of CREB and Bcl-xL (Figure 3D). In addition, expression of survivin—an inhibitor of apoptosis recently identified as a poor prognostic factor in NSCLC [27]—was reduced in Mer-knockdown cells. Modulation of this pro-survival signaling pathway was less robust and restricted to reduced expression of Bcl-xL and survivin in Axl-knockdown (shAxl8-G5) cells suggesting a possible explanation for the non-significant increase in YO-PRO and propidium iodide uptake reported in Figures 3B and 3C. Unexpectedly, expression of Bcl-2—typically considered a pro-survival factor—was absent in control A549 cells and upregulated in Mer-knockdown cells. This result suggests either pro-apoptotic function of Bcl-2 as previously described [28–31] or compensatory upregulation of Bcl-2 in response to Bcl-xL inhibition. Taken together, these findings indicate that Mer provides a survival advantage by stimulating the AKT/CREB/Bcl-xL/survivin signaling pathway in A549 cells.

Mer or Axl inhibition reduces NSCLC growth in vitro and in vivo

We hypothesized that inhibition of the anti-apoptotic signaling pathways activated downstream of Mer and Axl would reduce tumorigenic growth. Knockdown of Axl (shAxl8-G5) or Mer (shMer1-G8) significantly reduced the average number (16–17, $P < 0.05$) and size (344–377 μm, $P < 0.001$) of A549 colonies relative to shControl cells (32 colonies, 483 μm) (Fig. 4A). With the exception of shAxl8 cells, which produced smaller colonies (426 μm, $P < 0.05$), the polyclonal Axl- (shAxl8, shAxl9) and Mer-(shMer1, shMer4) knockdown cells did not exhibit differences in colony-forming capacity relative to the shControl population (Fig. 4A and data not shown). This effect is likely due to cell-to-cell variation in Mer and Axl expression levels in the polyclonal populations and more robust knockdown in the clonal populations. The growth-inhibitory phenotype of Mer and Axl inhibition was recapitulated by subcutaneous xenograft studies in nude mice (Fig. 4B). Axl knockdown reduced average tumor size (shAxl8-G5, 155 mm^3, $P = 0.0565$; shAxl9-D3, 159 mm^3, $P = 0.1135$) measured 47 days after injection when compared to shControl tumors (494 mm^3). Mer-knockdown (shMer1-G8) tumors were essentially immeasurable for the entire duration of the study (27 mm^3, $P = 0.002$ at day 47). These data support our hypothesis that inhibition of Mer or Axl is an effective anti-tumor strategy in NSCLC.

Mer or Axl knockdown enhances chemosensitivity of A549 cells by promoting apoptosis

Previous studies have suggested a role for Axl in mediating resistance to both targeted therapies [19, 32–34] and cytotoxic agents [35–37]. Studies from our laboratory demonstrated that Mer confers chemoresistance in leukemia and glioblastoma [38, 39]. Given our findings that Mer or Axl inhibition reduces NSCLC tumor growth, at least in part by promoting apoptosis, we hypothesized that Mer or Axl knockdown would improve the efficacy of cytotoxic agents by a similar mechanism. To test this hypothesis, control and Mer- or Axl-knockdown A549 cells were treated with cisplatin, carboplatin, doxorubicin, or etoposide, and relative cell numbers were determined by MTT assay (Fig. 5A). Mer or Axl knockdown resulted in 2-to 20-fold reductions in the half-maximal inhibitory concentrations (IC_{50}) of cisplatin and carboplatin relative to shControl cells (Table 2). In addition, Axl inhibition significantly improved A549 sensitivity to etoposide and doxorubicin.

The MTT assay measures metabolically active cells, and thus does not distinguish between the contributions of cell proliferation and cell death. We used the YO-PRO-1/PI assay to more specifically investigate whether Mer or Axl knockdown increased NSCLC cell death in response to treatment with cytotoxic agents. Axl-knockdown cells demonstrated a dose-dependent increase in apoptosis (39%–59%, $P < 0.01$) relative to shControl cells (24%–30%) following treatment with doxorubicin (Fig. 5B). A similar trend was observed when Axl-knockdown cells were treated with carboplatin. Consistent with the data in Figure 3, Mer-knockdown cells exhibited higher rates of basal apoptosis (36%, $P < 0.05$) than shControl cells (19%). In response to carboplatin, shMer1-G8 cells exhibited significantly more apoptotic cell death (53%, $P < 0.01$) than shControl cells (27%–31%). A similar trend was observed for doxorubicin-treated shMer1-G8 cells. Compared to shControl cells, both shMer1-G8 and shAxl8-G5 cells exhibited increased PARP cleavage in response to carboplatin and doxorubicin, confirming apoptotic pathway activation at the biochemical level (Fig. 5C). These data indicate that Mer and Axl inhibition increases NSCLC sensitivity to cytotoxic agents by promoting apoptosis and suggest additional mechanisms for Mer and Axl inhibitors.

Discussion

While tyrosine kinase inhibitors selective for mutated enzymes have highlighted the utility of targeted therapeutics in oncology, mechanisms apart from activating mutations—such as gene copy number variation, amplification, posttranscriptional regulation by miRNA, and autocrine or paracrine activation of overexpressed oncogenes—cause an oncogene to "drive" tumor development. Activating mutations in *Mer* and *Axl* have not been described. Evidence supporting alternative genetic mechanisms of TAM receptor-mediated oncogenesis is reviewed elsewhere [16]. This paper identifies Mer and Axl as RTKs that are frequently overexpressed in human NSCLC cells lines and tumors relative to surrounding normal lung tissue. Gas6, a ligand for Mer and Axl, is also frequently expressed by NSCLC cells and is found in plasma, suggesting that these RTKs are continuously activated in NSCLC via autocrine and/or paracrine mechanisms [40, 41]. This is the first report to describe a role for Mer in NSCLC and extends the findings of previous reports that have indicated a role for Axl in NSCLC. These results justify further investigation of Mer and Axl inhibitors as potential therapeutic agents in NSCLC.

Mer inhibition was an effective anti-tumor strategy in A549 cells despite relatively low expression of Mer suggesting that total Mer or Axl levels may not be the optimal means to identify patients who might benefit from Mer- and/or Axl-targeted agents. A more likely predictive biomarker might be relative phosphorylation levels of Mer and Axl, which were high in A549 cells. Although Mer phosphorylation can be difficult to detect and often requires application of pervanadate to stabilize the signal, we are currently investigating the utility of various assay platforms—including traditional immunohistochemistry as well as new ELISA-based methods—to reliably measure Mer phosphorylation in xenograft and clinical samples. The new ELISA-based technology provides considerably improved sensitivity relative to traditional western blotting and may permit assessment of Mer phosphorylation in clinical samples without pervanadate treatment. Alternatively, a specific tumor gene expression profile might be considered. In addition, Gas6, soluble Axl, and

soluble Mer have been measured in human serum and may have prognostic value in autoimmune disease and cancer [42–45]. Preclinical investigation of translational Mer and Axl inhibitors is necessary before the predictive value of these and other biomarkers can be assessed in the clinic.

Contrary to our findings, Axl positivity was previously identified as a poor prognostic factor in lung adenocarcinoma [20]. In that report, tumors were defined as Axl-positive if more than 25% of the cells were stained by Axl immunohistochemistry; however, staining intensity was not evaluated. Our analysis differs in that the H-Score represents the percentage of positive cells and staining intensity. Both parameters are informative when assessing protein expression within tumor tissues. In this study, the majority of NSCLC tumors exhibited overexpression of Mer (69%) and/or Axl (93%) relative to surrounding normal lung tissue where expression of both receptors was completely absent. Similar patterns were observed in vitro with overexpression of Mer and Axl protein in 92% and 69%, respectively, of NSCLC cell lines relative to NHBE cells. Analysis of receptor phosphorylation patterns revealed that when present, both Mer and Axl tend to be phosphorylated under normal culture conditions (Axl in 5/5 cell lines and Mer in 6/7 cell lines). This effect could be related to the presence of Gas6 or another TAM receptor ligand in the serum added to culture media. Receptor phosphorylation was detected in some cells lines (Mer in Colo699 and Axl in A549, H2009, and HCC15) even after removal of serum from the culture medium, suggesting that these cells may express Gas6 or another TAM ligand. Future studies should evaluate the phosphorylation status of Mer and Axl in NSCLC tumor tissues to investigate whether activation of the two receptors frequently occurs together, and whether these particular phenotypes have prognostic or predictive value.

Previous studies have delineated MAPK/p38/ERK and PI3K/AKT signaling pathways activated downstream of Mer and Axl, and roles for these RTKs in cell survival and proliferation are well established [15, 38, 39, 46–49]. This is the first report to document activation of these Mer and Axl signaling pathways in lung cancer cells. This is also the first paper to extend the TAM receptor-activated MAPK pathway to include the downstream effectors MSK1/2, CREB, and ATF1. A recent study identified a CREB-binding motif in the *Axl* promoter region of leukemia cells [50], suggesting that constitutive activation of the MAPK and/or AKT pathways downstream of Mer and Axl may drive overexpression of Axl, at least in some cancer cell types. Phosphorylation of GSK3α/β has been previously described in response to Gas6 but expression of the TAM family receptors was not fully characterized and thus the upstream receptor involved was not determined [51–53]. Differentiation of signaling pathways downstream of individual TAM receptors is complicated by the fact that most cell lines express more than one family member. In addition, antibodies that reliably detect the third family member, Tyro3, were not available until recently. Although the Mer-positive Colo699 cell line does not express Axl at the protein or mRNA level, these cells—as well as several other NSCLC cell lines—express Tyro3 (Supplementary Fig. 3). We used the Mer- and Axl-knockdown A549 cell lines to explore differences in pro-survival signaling mechanisms downstream of Mer and Axl. Our results suggest that Mer inhibition induces apoptosis by attenuating pro-survival signaling mechanisms mediated by AKT, CREB, Bcl-xL, and survivin. Axl inhibition exhibited less

robust modulation of this pathway as demonstrated by reduced Bcl-xL and survivin expression without inhibition of AKT or CREB. A minimal threshold of Axl expression may be required for inhibition of this pro-survival pathway as Bcl-xL and survivin expression was not altered in shControl cells although they exhibited a smaller, but measureable, reduction in Axl expression relative to Axl-knockdown cells in these experiments. Expression of Bcl-2 was absent in control and Axl-knockdown A549 cells but upregulated in Mer-knockdown cells. Although Bcl-2 most commonly exhibits pro-survival function, a growing body of evidence demonstrates that this protein is also capable of inducing apoptosis [28, 30, 54], particularly when expressed at high levels or bound to an orphan nuclear receptor [29, 31]. These findings highlight specific differences in pro-survival signaling mechanisms activated downstream of Mer and Axl in the A549 cell line and may contribute to the different functional outcomes observed in Mer-knockdown and Axl-knockdown cells. Development of novel biologic or small molecule inhibitors that selectively inhibit a single TAM receptor will be useful tools for elucidation of additional signaling pathways that are unique to individual TAM receptors. The data presented here expand our understanding of TAM receptor function at the biochemical level and reveal novel pathway interactions that may be useful as surrogate markers for Mer and Axl inhibition in lung cancer cells.

Axl has been shown to mediate migration and invasion of glioblastoma, lung cancer, and breast cancer cells [18, 20, 55, 56]. The Axl-stimulated signaling pathways that mediate this phenotype may include upregulation of matrix metalloproteinases and transition of solid tumor cells from an epithelial to mesenchymal morphology [17, 57, 58]. Axl/Gas6 signaling via Rho family GTPases regulates actin dynamics and migration of specialized neurons [47, 59], but these pathways have not been investigated downstream of Axl in cancer cells. However, Mer was recently shown to regulate migration of glioblastoma cells via altered FAK and Rho signaling [60]. This novel finding is consistent with previous reports that established roles for FAK and Rho GTPases in Mer-mediated morphological changes required for phagocytic engulfment of apoptotic cells [49, 61, 62]. Thus, additional studies investigating the role of Mer in NSCLC migration are warranted.

Our data clearly demonstrate that Mer inhibition has profound functional consequences in lung cancer cells. Mer-knockdown cells exhibited higher rates of apoptosis, and tumor growth was significantly reduced in colony formation assays. More impressively, this effect was recapitulated in mice: growth of xenograft tumors was completely blocked by Mer knockdown. This study is the first to demonstrate a role for Mer in NSCLC and validate Mer as a novel therapeutic target in NSCLC.

As mentioned above, previous studies identified Axl as a therapeutic target in NSCLC [18–20]. Our results support and expand these findings by demonstrating that Axl knockdown inhibits NSCLC growth in vitro and in vivo, and suggests that Axl inhibition may enhance the antitumor effects of chemotherapeutic agents by promoting apoptosis. Interestingly, Mer knockdown was a more effective inhibitor of tumor growth than Axl knockdown, suggesting that Mer plays a more substantial role than Axl in NSCLC tumor progression. Although Mer knockdown improved chemosensitivity, this phenotype was limited to the platinum agents and the IC50 reductions were smaller in magnitude compared to those observed with Axl knockdown. Upon treatment with cytotoxic agents, Mer-knockdown and Axl-knockdown

cells exhibited similar levels of apoptotic cell death and PARP cleavage suggesting that the differences in IC50 values observed in the MTT assay may be due to Axl inhibition of another cellular mechanism such as cell proliferation. Taken together, these data suggest that Mer may play a more prominent role in cell survival and tumor progression while Axl may be more involved in cell proliferation and chemoresistance. Strategies targeting both Mer and Axl may therefore work by multiple mechanisms and be most effective.

Regardless of whether Mer and Axl play individual or concerted roles in NSCLC, these data conclusively demonstrate that clinically translatable compounds inhibiting Mer and/or Axl merit further investigation as potential therapeutics in NSCLC. We are currently investigating an inhibitory anti-Mer monoclonal antibody and a series of novel Mer- and Axl-selective small molecule tyrosine kinase inhibitors in mouse models of NSCLC. A number of other drugs with activity against Mer and/or Axl are in various phases of development (reviewed in ref. 17).

Materials and Methods

Clinical samples and immunohistochemistry

De-identified clinical specimens of primary tumors were assembled into a tissue microarray (TMA) by the University of Colorado Cancer Center (UCCC) SPORE in lung cancer tissue bank core [22]. The study protocol was approved by the Colorado Multiple Institution Review Board. The TMA contains samples from patients diagnosed with NSCLC at the UCCC and the Johns Hopkins Medical Institution between 1993 and 1999. Only samples from patients diagnosed at the UCCC were included in this study because clinical follow-up information was updated in 2008. To assess expression of Mer and Axl proteins in the clinical samples, we used an enzyme-based staining method whereby binding of horseradish peroxidase-conjugated antibodies is visualized by oxidation of a reporter dye (3, 3′ diaminobenzidene, DAB). Details are provided in the Supplementary Information.

All specimens were scored independently by two board-certified pathologists (D.T.M. and P.J.). An H-Score was calculated for each specimen by multiplying the percentage of positive tumor cells (0% to 100%) by the dominant staining intensity (scale 0 to 4). Thus, the possible range of H-Scores was 0 to 400. When the reliability of a single reader's scores was evaluated, the intraclass correlation coefficients [63] for Axl and Mer were moderately high (0.74 and 0.65, respectively), indicating that the agreement between the two pathologists was good. The correlation coefficients measuring reliability of using the mean ratings were relatively high (0.85 for Axl and 0.79 for Mer) indicating excellent agreement between raters. Based on these two results we used the average scores of the two pathologists.

Cell culture and reagents

NHBE cells (also known as HBEC-3KT [64]) were cultured in bronchial epithelial cell growth medium (Lonza, CC-3170). The NSCLC cell lines were cultured in RPMI medium supplemented with 10% fetal bovine serum, penicillin (100 U/ml) and streptomycin (100 μg/ml). Cell line sources and authentication details are provided in the Supplemental

Information. Recombinant human (rhGas6, 885-GS) and mouse (rmGas6, 986-GS) growth arrest specific 6 (Gas6) were purchased from R&D Systems and reconstituted in PBS. Carboplatin (C2538), cisplatin (P4394), and doxorubicin (D1515) were from Sigma. Etoposide (341205) was obtained from Calbiochem.

Animals and subcutaneous xenograft model

All experiments involving mice were approved by the University of Colorado Institutional Animal Care and Use Committee. Subconfluent cultures of A549 cells were washed with sterile PBS and resuspended at 2×10^7 cells/ml in PBS. Male and female athymic nude mice (aged 5–9 weeks) received 100 μl of cell suspension via subcutaneous injection in the left or right flank. Engraftment typically occurred 18–21 days after injection. Beginning on day 19, tumors were measured twice weekly with calipers and tumor volume (*V*) was calculated using the formula $V = \pi a^2 b/6$, where *a* represents the shortest diameter measured perpendicular to the longest diameter (*b*).

Western blotting and phospho-kinase array

Whole-cell lysates were prepared in lysis buffer (50 mM HEPES pH 7.5, 150 mM NaCl, 10 mM EDTA, 10% glycerol, 1% Triton X-100, 1 mM Na_3VO_4, 0.1 mM Na_2MoO_4) supplemented with protease inhibitors (Complete Mini, Roche Molecular Biochemicals). Total protein concentrations were determined using the Bio-Rad Protein Assay and samples were analyzed by sodium dodecyl sulfate-polyacrylamide gel electrophoresis and immunoblotting. The protein-kinase array (R&D Systems, ARY003) was performed according to manufacturer guidelines. All antibodies used for immunoblotting were applied as recommended by the manufacturer. Vendor catalog numbers are provided in the Supplementary Information.

Immunoprecipitation and detection of phosphorylated Mer and Axl

Phosphorylation of Mer is difficult to measure, possibly due to phosphatases in complex with Mer that result in extreme lability of Mer phosphorylation. We developed a phospho-Mer assay whereby cells are treated with pervanadate (0.12 mM Na_3VO_4 in 0.002% H_2O_2) for 1–2 minutes prior to cell lysis to preserve the phosphorylation status of Mer. Because pervanadate treatment precludes assessment of downstream signaling events (data not shown) this procedure was strictly limited to analysis of Mer and Axl phosphorylation. Mer was immunoprecipitated from pervanadate-treated lysates by incubating with mouse monoclonal anti-Mer antibody (R&D Systems, MAB8912) followed by incubation with rec-Protein G-sepharose 4B (Invitrogen, 10–1242) bead slurry. Immune complexes were collected by centrifugation and washed with lysis buffer. Beads were resuspended in Laemmli buffer (62.5 mM Tri-HCl pH 6.8, 25% glycerol, 5% β-mercaptoethanol, 2% SDS, and 0.01% bromophenol blue) and boiled prior to analysis by western blotting. Axl was immunoprecipitated from the same samples by incubating the supernatant of Mer immunoprecipitates with goat polyclonal anti-Axl (R&D Systems, AF154) and subsequently following the same protocol.

Quantitative Reverse Transcription PCR

Diluted RNA (50 ng/reaction or 5 ng/reaction) was used as a template for real time RT-PCR in the presence of primer pairs homologous to Mer or Axl and GAPDH, respectively. Primer and probe sequences and concentrations are provided in the Supplementary Information. Threshold cycle values (C_t) from at least three independent experiments performed in triplicate were normalized to the GAPDH internal control using the equation $\Delta C_t = C_{t\ \text{Mer or Axl}} - C_{t\ \text{GAPDH}}$. Standard curves were generated with multiple cell lines, which demonstrated >99% efficiency of all three primer/probe sets. Thus, a two-fold difference in RNA concentration per cycle was assumed for calculation of relative expression levels.

Lentiviral transduction and isolation of clonal populations

Lentiviral vectors (pLKO.1) containing shRNA sequences targeting Mer (shMer1, Oligo ID: TRCN0000000862 and shMer4, Oligo ID: TRCN0000000865), Axl (shAxl8, Oligo ID: TRCN0000000574 and shAxl9, Oligo ID: TRCN0000000575), or GFP (RHS4459) were obtained from Open Biosystems. The GFP vector, which does not express the fluorescent protein, encodes an shRNA that engages the endogenous RNAi machinery and targets GFP mRNA; since human cells do not express GFP, this vector serves as a non-silencing control and is referred to as “shControl” throughout the text. Lentiviral particles were produced using the 293FT cell line and the third generation packaging system developed by the laboratory of Dr. Didier Trono. Target cells were incubated in media containing viral particles and 8 μg/ml hexadimethrine bromide (Sigma-Aldrich) for 1 hour at room temperature. Cells were then cultured overnight and incubation with viral media was repeated the following day to increase transduction efficiency. Cells were cultured overnight prior to selection in media containing 2 μg/ml puromycin (Clontech). Puromycin resistant colonies were typically observed 5–9 days after transduction. Polyclonal populations were maintained in puromycin to prevent loss of knockdown. Stable clonal isolates were obtained by single-cell flow cytometry sorting and maintained in normal culture media.

Clonogenic colony formation assay

A549 cells were plated in triplicate wells of 6-well dishes at ultra-low density (50 cells/well) and cultured under normal conditions without perturbation for seven days. Colonies were washed with PBS and stained with crystal violet (0.5% w/v in 25% methanol). Stained plates were rinsed in dH_2O and allowed to dry at room temperature. Colony diameter and number was quantified using a GelCount colony counter and software (v1.4, Oxford Optronix). Only colonies containing > 50 cells were analyzed [65].

YO-PRO-1/propidium iodide assay of apoptosis and cell death

Subconfluent cultures of A549 cells were treated as indicated in the figure legends. Cells were lifted with 0.02% EDTA in PBS, combined with culture supernatants, and centrifuged for 5 minutes at 950*g*. Cell pellets were resuspended in PBS containing 0.2 μM YO-PRO-1 (Invitrogen, Y3603) and 1.5 μM propidium iodide (PI) (Invitrogen, P3566). Uptake of YO-PRO-1 and PI was measured using a FC500 flow cytometer and CXP analysis software (Beckman Coulter). Cells undergoing apoptosis are stained with YO-PRO-1 but are

impermeable to PI. Dead cells and cells in late apoptosis are permeable to both dyes. Viable cells are not stained by either dye.

Colorimetric assay of relative cell number

A549 cells were seeded into 96-well plates at a density of 2.5×10^4 cells/cm^2. Cells were allowed to adhere overnight before addition of cytotoxic agents or vehicle for an additional 48 hours. MTT (3-(4,5-Dimethyl-2-thiazolyl)-2,5-diphenyl-2H-tetrazolium bromide, Sigma-Aldrich) was added and cells were cultured for an additional four hours. Solubilization solution (2X, 10% sodium dodecyl sulfate in 0.01 M HCl) was added and plates were incubated at 37°C overnight. Optical density was determined at 562 nm with a reference wavelength of 650 nm. Relative cell numbers were calculated by subtraction of background absorbance and normalization to untreated controls.

Statistical Analysis

All data are representative of three independent experiments unless otherwise noted. Statistical analyses of immunohistochemistry data were performed by the University of Colorado Biostatistics and Bioinformatics Core using SAS/BASE and SAS/STAT software, Version 9.2 of the SAS System for Windows (SAS Institute Inc.). Descriptive statistics were calculated. Continuous variables were categorized: age at diagnosis was dichotomized at its median 62-years; Mer H-Score and Axl H-Score were categorized according to convention [22]. For clinical characteristics (age at diagnosis, histology, and sex), statistical significance between different levels of each characteristic was assessed by log-rank test. On stage, categorical Axl H-Score, and categorical Mer H-Score, statistical significance between different levels of each factor was assessed by log-rank test for trend as these variables are considered ordinal. Statistical analyses of all other data were performed using Prism 5 (Version 5.04, GraphPad Software, Inc.).

Supplementary Material

Refer to Web version on PubMed Central for supplementary material.

Acknowledgments

Financial Support: This work was supported in part by grants from Uniting Against Lung Cancer: Elliot's Legacy (RMAL), the Lung Cancer Research Foundation (RMAL), the American Cancer Society (RSG-08-291-01-LIB, DKG), and the National Institutes of Health (RO1CA137078, DKG). RMA Linger received a Career Development Award from the University of Colorado Cancer Center SPORE in Lung Cancer (NIH 5P50CA058187). DK Graham is the Damon Runyon-Novartis Clinical Investigator supported (in part) by the Damon Runyon Cancer Research Foundation (CI-39-07).

This work was supported in part by grants from Uniting Against Lung Cancer: Elliot's Legacy (RMAL), the Lung Cancer Research Foundation (RMAL), the American Cancer Society (RSG-08-291-01-LIB, DKG), and the National Institutes of Health (RO1CA137078, DKG). RMA Linger received a Career Development Award from the University of Colorado Cancer Center SPORE in Lung Cancer (NIH 5P50CA058187). DK Graham is the Damon Runyon-Novartis Clinical Investigator supported (in part) by the Damon Runyon Cancer Research Foundation (CI-39-07). The authors wish to thank Karen Helm, Christine Childs, and Lester Acosta in the University of Colorado Cancer Center Flow Cytometry Core for their expert technical assistance, Randall Wong in the University of Colorado Denver Diabetes & Endocrinology Research Center Molecular Biology Core Facility (NIH P30 DK57516) for cell line authentication services, Patricia Lenhart for help optimizing Mer and Axl immunohistochemistry of human tissues, and Storey Wilson and Andrea Abeyta for technical assistance with the Aperio imaging system used to digitize stained tumor microarray slides.

References

1. Society AC. Cancer Facts & Figures 2012. Atlanta: American Cancer Society; 2012.
2. SEER Cancer Statistics Review, 1975–2008 [database on the Internet]. National Cancer Institute; 2011. [cited 1/25/2012]. Available from: http://seer.cancer.gov/csr/1975_2008/
3. Shaw AT, Yeap BY, Solomon BJ, Riely GJ, Gainor J, Engelman JA, et al. Effect of crizotinib on overall survival in patients with advanced non-small-cell lung cancer harbouring ALK gene rearrangement: a retrospective analysis. Lancet Oncol. 2011; 12(11):1004–12. [PubMed: 21933749]
4. Mok TS, Wu YL, Thongprasert S, Yang CH, Chu DT, Saijo N, et al. Gefitinib or carboplatin-paclitaxel in pulmonary adenocarcinoma. N Engl J Med. 2009; 361(10):947–57. [PubMed: 19692680]
5. Paik PK, Arcila ME, Fara M, Sima CS, Miller VA, Kris MG, et al. Clinical characteristics of patients with lung adenocarcinomas harboring BRAF mutations. J Clin Oncol. 2011; 29(15):2046–51. [PubMed: 21483012]
6. Brose MS, Volpe P, Feldman M, Kumar M, Rishi I, Gerrero R, et al. BRAF and RAS mutations in human lung cancer and melanoma. Cancer Res. 2002; 62(23):6997–7000. [PubMed: 12460918]
7. Yamamoto H, Shigematsu H, Nomura M, Lockwood WW, Sato M, Okumura N, et al. PIK3CA mutations and copy number gains in human lung cancers. Cancer Res. 2008; 68(17):6913–21. [PubMed: 18757405]
8. Shigematsu H, Takahashi T, Nomura M, Majmudar K, Suzuki M, Lee H, et al. Somatic mutations of the HER2 kinase domain in lung adenocarcinomas. Cancer Res. 2005; 65(5):1642–6. [PubMed: 15753357]
9. Engelman JA, Zejnullahu K, Gale CM, Lifshits E, Gonzales AJ, Shimamura T, et al. PF00299804, an irreversible pan-ERBB inhibitor, is effective in lung cancer models with EGFR and ERBB2 mutations that are resistant to gefitinib. Cancer Res. 2007; 67(24):11924–32. [PubMed: 18089823]
10. Engelman JA, Chen L, Tan X, Crosby K, Guimaraes AR, Upadhyay R, et al. Effective use of PI3K and MEK inhibitors to treat mutant Kras G12D and PIK3CA H1047R murine lung cancers. Nat Med. 2008; 14(12):1351–6. [PubMed: 19029981]
11. Pratilas CA, Hanrahan AJ, Halilovic E, Persaud Y, Soh J, Chitale D, et al. Genetic predictors of MEK dependence in non-small cell lung cancer. Cancer Res. 2008; 68(22):9375–83. [PubMed: 19010912]
12. Sunaga N, Shames DS, Girard L, Peyton M, Larsen JE, Imai H, et al. Knockdown of oncogenic KRAS in non-small cell lung cancers suppresses tumor growth and sensitizes tumor cells to targeted therapy. Mol Cancer Ther. 2011; 10(2):336–46. [PubMed: 21306997]
13. Wallin JJ, Edgar KA, Guan J, Berry M, Prior WW, Lee L, et al. GDC-0980 is a novel class I PI3K/mTOR kinase inhibitor with robust activity in cancer models driven by the PI3K pathway. Mol Cancer Ther. 2011; 10(12):2426–36. [PubMed: 21998291]
14. Janku F, Garrido-Laguna I, Petruzelka LB, Stewart DJ, Kurzrock R. Novel therapeutic targets in non-small cell lung cancer. J Thorac Oncol. 2011; 6(9):1601–12. [PubMed: 21849857]
15. Linger RMA, Keating AK, Earp HS, Graham DK. TAM receptor tyrosine kinases: biologic functions, signaling, and potential therapeutic targeting in human cancer. Adv Cancer Res. 2008; 100:35–83. [PubMed: 18620092]
16. Brandao L, Migdall-Wilson J, Eisenman K, Graham DK. TAM Receptors in Leukemia: Expression, Signaling, and Therapeutic Implications. Critical reviews in oncogenesis. 2011; 16(1–2):47–63. [PubMed: 22150307]
17. Linger RM, Keating AK, Earp HS, Graham DK. Taking aim at Mer and Axl receptor tyrosine kinases as novel therapeutic targets in solid tumors. Expert Opin Ther Targets. 2010; 14(10):1073–90. [PubMed: 20809868]
18. Li Y, Ye X, Tan C, Hongo JA, Zha J, Liu J, et al. Axl as a potential therapeutic target in cancer: role of Axl in tumor growth, metastasis and angiogenesis. Oncogene. 2009; 28(39):3442–55. [PubMed: 19633687]
19. Ye X, Li Y, Stawicki S, Couto S, Eastham-Anderson J, Kallop D, et al. An anti-Axl monoclonal antibody attenuates xenograft tumor growth and enhances the effect of multiple anticancer therapies. Oncogene. 2010; 29(38):5254–64. [PubMed: 20603615]

20. Shieh YS, Lai CY, Kao YR, Shiah SG, Chu YW, Lee HS, et al. Expression of axl in lung adenocarcinoma and correlation with tumor progression. Neoplasia. 2005; 7(12):1058–64. [PubMed: 16354588]
21. Rikova K, Guo A, Zeng Q, Possemato A, Yu J, Haack H, et al. Global survey of phosphotyrosine signaling identifies oncogenic kinases in lung cancer. Cell. 2007; 131(6):1190–203. [PubMed: 18083107]
22. Bremnes RM, Veve R, Gabrielson E, Hirsch FR, Baron A, Bemis L, et al. High-throughput tissue microarray analysis used to evaluate biology and prognostic significance of the E-cadherin pathway in non-small-cell lung cancer. J Clin Oncol. 2002; 20(10):2417–28. [PubMed: 12011119]
23. Roux PP, Blenis J. ERK and p38 MAPK-activated protein kinases: a family of protein kinases with diverse biological functions. Microbiol Mol Biol Rev. 2004; 68(2):320–44. [PubMed: 15187187]
24. Aggarwal S, Kim SW, Ryu SH, Chung WC, Koo JS. Growth suppression of lung cancer cells by targeting cyclic AMP response element-binding protein. Cancer Res. 2008; 68(4):981–8. [PubMed: 18281471]
25. Reeve JG, Xiong J, Morgan J, Bleehen NM. Expression of apoptosis-regulatory genes in lung tumour cell lines: relationship to p53 expression and relevance to acquired drug resistance. Br J Cancer. 1996; 73(10):1193–200. [PubMed: 8630278]
26. Pugazhenthi S, Nesterova A, Sable C, Heidenreich KA, Boxer LM, Heasley LE, et al. Akt/protein kinase B up-regulates Bcl-2 expression through cAMP-response element-binding protein. J Biol Chem. 2000; 275(15):10761–6. [PubMed: 10753867]
27. Zhang LQ, Wang J, Jiang F, Xu L, Liu FY, Yin R. Prognostic value of survivin in patients with non-small cell lung carcinoma: a systematic review with meta-analysis. PLoS One. 2012; 7(3):e34100. [PubMed: 22457815]
28. Arriola EL, Rodriguez-Lopez AM, Hickman JA, Chresta CM. Bcl-2 overexpression results in reciprocal downregulation of Bcl-X(L) and sensitizes human testicular germ cell tumours to chemotherapy-induced apoptosis. Oncogene. 1999; 18(7):1457–64. [PubMed: 10050882]
29. Lin B, Kolluri SK, Lin F, Liu W, Han YH, Cao X, et al. Conversion of Bcl-2 from protector to killer by interaction with nuclear orphan receptor Nur77/TR3. Cell. 2004; 116(4):527–40. [PubMed: 14980220]
30. Oliver L, Hue E, Rossignol J, Bougras G, Hulin P, Naveilhan P, et al. Distinct roles of Bcl-2 and Bcl-Xl in the apoptosis of human bone marrow mesenchymal stem cells during differentiation. PLoS One. 2011; 6(5):e19820. [PubMed: 21589877]
31. Shinoura N, Yoshida Y, Nishimura M, Muramatsu Y, Asai A, Kirino T, et al. Expression level of Bcl-2 determines anti- or proapoptotic function. Cancer Res. 1999; 59(16):4119–28. [PubMed: 10463617]
32. Grosso S, Puissant A, Dufies M, Colosetti P, Jacquel A, Lebrigand K, et al. Gene expression profiling of imatinib and PD166326-resistant CML cell lines identifies Fyn as a gene associated with resistance to BCR-ABL inhibitors. Mol Cancer Ther. 2009; 8(7):1924–33. [PubMed: 19567819]
33. Liu L, Greger J, Shi H, Liu Y, Greshock J, Annan R, et al. Novel mechanism of lapatinib resistance in HER2-positive breast tumor cells: activation of AXL. Cancer Res. 2009; 69(17): 6871–8. [PubMed: 19671800]
34. Mahadevan D, Cooke L, Riley C, Swart R, Simons B, Della Croce K, et al. A novel tyrosine kinase switch is a mechanism of imatinib resistance in gastrointestinal stromal tumors. Oncogene. 2007; 26(27):3909–19. [PubMed: 17325667]
35. Holland SJ, Pan A, Franci C, Hu Y, Chang B, Li W, et al. R428, a Selective Small Molecule Inhibitor of Axl Kinase, Blocks Tumor Spread and Prolongs Survival in Models of Metastatic Breast Cancer. Cancer Res. 2010; 70(4):1544–54. [PubMed: 20145120]
36. Hong CC, Lay JD, Huang JS, Cheng AL, Tang JL, Lin MT, et al. Receptor tyrosine kinase AXL is induced by chemotherapy drugs and overexpression of AXL confers drug resistance in acute myeloid leukemia. Cancer Lett. 2008; 268(2):314–24. [PubMed: 18502572]
37. Macleod K, Mullen P, Sewell J, Rabiasz G, Lawrie S, Miller E, et al. Altered ErbB receptor signaling and gene expression in cisplatin-resistant ovarian cancer. Cancer Res. 2005; 65(15): 6789–800. [PubMed: 16061661]

38. Keating AK, Kim GK, Jones AE, Donson AM, Ware K, Mulcahy JM, et al. Inhibition of Mer and Axl receptor tyrosine kinases in astrocytoma leads to increased apoptosis and improved chemosensitivity. Mol Cancer Ther. 2010; 9(5):1298–307. [PubMed: 20423999]

39. Keating AK, Salzberg DB, Sather S, Liang X, Nickoloff S, Anwar A, et al. Lymphoblastic leukemia/lymphoma in mice overexpressing the Mer (MerTK) receptor tyrosine kinase. Oncogene. 2006; 25(45):6092–100. [PubMed: 16652142]

40. Wimmel A, Glitz D, Kraus A, Roeder J, Schuermann M. Axl receptor tyrosine kinase expression in human lung cancer cell lines correlates with cellular adhesion. Eur J Cancer. 2001; 37(17):2264–74. [PubMed: 11677117]

41. Balogh I, Hafizi S, Stenhoff J, Hansson K, Dahlback B. Analysis of Gas6 in human platelets and plasma. Arterioscler Thromb Vasc Biol. 2005; 25(6):1280–6. [PubMed: 15790929]

42. Gustafsson A, Martuszewska D, Johansson M, Ekman C, Hafizi S, Ljungberg B, et al. Differential expression of Axl and Gas6 in renal cell carcinoma reflecting tumor advancement and survival. Clin Cancer Res. 2009; 15(14):4742–9. [PubMed: 19567592]

43. Jansen FH, van Rijswijk A, Teubel W, van Weerden WM, Reneman S, van den Bemd GJ, et al. Profiling of Antibody Production against Xenograft-released Proteins by Protein Microarrays Discovers Prostate Cancer Markers. J Proteome Res. 2011

44. Wu J, Ekman C, Jonsen A, Sturfelt G, Bengtsson AA, Gottsater A, et al. Increased plasma levels of the soluble Mer tyrosine kinase receptor in systemic lupus erythematosus relate to disease activity and nephritis. Arthritis research & therapy. 2011; 13(2):R62. [PubMed: 21496228]

45. Ekman C, Jonsen A, Sturfelt G, Bengtsson AA, Dahlback B. Plasma concentrations of Gas6 and sAxl correlate with disease activity in systemic lupus erythematosus. Rheumatology (Oxford). 2011; 50(6):1064–9. [PubMed: 21278074]

46. Shankar SL, O'Guin K, Kim M, Varnum B, Lemke G, Brosnan CF, et al. Gas6/Axl signaling activates the phosphatidylinositol 3-kinase/Akt1 survival pathway to protect oligodendrocytes from tumor necrosis factor alpha-induced apoptosis. J Neurosci. 2006; 26(21):5638–48. [PubMed: 16723520]

47. Allen MP, Linseman DA, Udo H, Xu M, Schaack JB, Varnum B, et al. Novel mechanism for gonadotropin-releasing hormone neuronal migration involving Gas6/Ark signaling to p38 mitogen-activated protein kinase. Mol Cell Biol. 2002; 22(2):599–613. [PubMed: 11756555]

48. Allen MP, Xu M, Linseman DA, Pawlowski JE, Bokoch GM, Heidenreich KA, et al. Adhesion-related kinase repression of gonadotropin-releasing hormone gene expression requires Rac activation of the extracellular signal-regulated kinase pathway. J Biol Chem. 2002; 277(41): 38133–40. [PubMed: 12138087]

49. Guttridge KL, Luft JC, Dawson TL, Kozlowska E, Mahajan NP, Varnum B, et al. Mer receptor tyrosine kinase signaling: prevention of apoptosis and alteration of cytoskeletal architecture without stimulation or proliferation. J Biol Chem. 2002; 277(27):24057–66. [PubMed: 11929866]

50. Mudduluru G, Leupold JH, Stroebel P, Allgayer H. PMA up-regulates the transcription of Axl by AP-1 transcription factor binding to TRE sequences via the MAPK cascade in leukaemia cells. Biology of the cell/under the auspices of the European Cell Biology Organization. 2011; 103(1): 21–33. [PubMed: 20977427]

51. Demarchi F, Verardo R, Varnum B, Brancolini C, Schneider C. Gas6 anti-apoptotic signaling requires NF-kappa B activation. J Biol Chem. 2001; 276(34):31738–44. [PubMed: 11425860]

52. Goruppi S, Chiaruttini C, Ruaro ME, Varnum B, Schneider C. Gas6 induces growth, beta-catenin stabilization, and T-cell factor transcriptional activation in contact-inhibited C57 mammary cells. Mol Cell Biol. 2001; 21(3):902–15. [PubMed: 11154277]

53. Alciato F, Sainaghi PP, Sola D, Castello L, Avanzi GC. TNF-alpha, IL-6, and IL-1 expression is inhibited by GAS6 in monocytes/macrophages. J Leukoc Biol. 2010; 87(5):869–75. [PubMed: 20103767]

54. Han Z, Chatterjee D, Early J, Pantazis P, Hendrickson EA, Wyche JH. Isolation and characterization of an apoptosis-resistant variant of human leukemia HL-60 cells that has switched expression from Bcl-2 to Bcl-xL. Cancer Res. 1996; 56(7):1621–8. [PubMed: 8603411]

55. Vajkoczy P, Knyazev P, Kunkel A, Capelle HH, Behrndt S, von Tengg-Kobligk H, et al. Dominant-negative inhibition of the Axl receptor tyrosine kinase suppresses brain tumor cell

growth and invasion and prolongs survival. Proc Natl Acad Sci U S A. 2006; 103(15):5799–804. [PubMed: 16585512]

56. Zhang YX, Knyazev PG, Cheburkin YV, Sharma K, Knyazev YP, Orfi L, et al. AXL is a potential target for therapeutic intervention in breast cancer progression. Cancer Res. 2008; 68(6):1905–15. [PubMed: 18339872]
57. Gjerdrum C, Tiron C, Hoiby T, Stefansson I, Haugen H, Sandal T, et al. Axl is an essential epithelial-to-mesenchymal transition-induced regulator of breast cancer metastasis and patient survival. Proc Natl Acad Sci U S A. 2010; 107(3):1124–9. [PubMed: 20080645]
58. Tai KY, Shieh YS, Lee CS, Shiah SG, Wu CW. Axl promotes cell invasion by inducing MMP-9 activity through activation of NF-kappaB and Brg-1. Oncogene. 2008; 27(29):4044–55. [PubMed: 18345028]
59. Nielsen-Preiss SM, Allen MP, Xu M, Linseman DA, Pawlowski JE, Bouchard RJ, et al. Adhesion-related kinase induction of migration requires phosphatidylinositol-3-kinase and ras stimulation of rac activity in immortalized gonadotropin-releasing hormone neuronal cells. Endocrinology. 2007; 148(6):2806–14. [PubMed: 17332061]
60. Rogers AE, Le JP, Sather S, Pernu BM, Graham DK, Pierce AM, et al. Mer receptor tyrosine kinase inhibition impedes glioblastoma multiforme migration and alters cellular morphology. Oncogene. 2011
61. Scott RS, McMahon EJ, Pop SM, Reap EA, Caricchio R, Cohen PL, et al. Phagocytosis and clearance of apoptotic cells is mediated by MER. Nature. 2001; 411(6834):207–11. [PubMed: 11346799]
62. Wu Y, Singh S, Georgescu MM, Birge RB. A role for Mer tyrosine kinase in alphavbeta5 integrin-mediated phagocytosis of apoptotic cells. J Cell Sci. 2005; 118(Pt 3):539–53. [PubMed: 15673687]
63. Shrout PE, Fleiss JL. Intraclass correlations: uses in assessing rater reliability. Psychol Bull. 1979; 86(2):420–8. [PubMed: 18839484]
64. Ramirez RD, Sheridan S, Girard L, Sato M, Kim Y, Pollack J, et al. Immortalization of human bronchial epithelial cells in the absence of viral oncoproteins. Cancer Res. 2004; 64(24):9027–34. [PubMed: 15604268]
65. Franken NA, Rodermond HM, Stap J, Haveman J, van Bree C. Clonogenic assay of cells in vitro. Nat Protoc. 2006; 1(5):2315–9. [PubMed: 17406473]

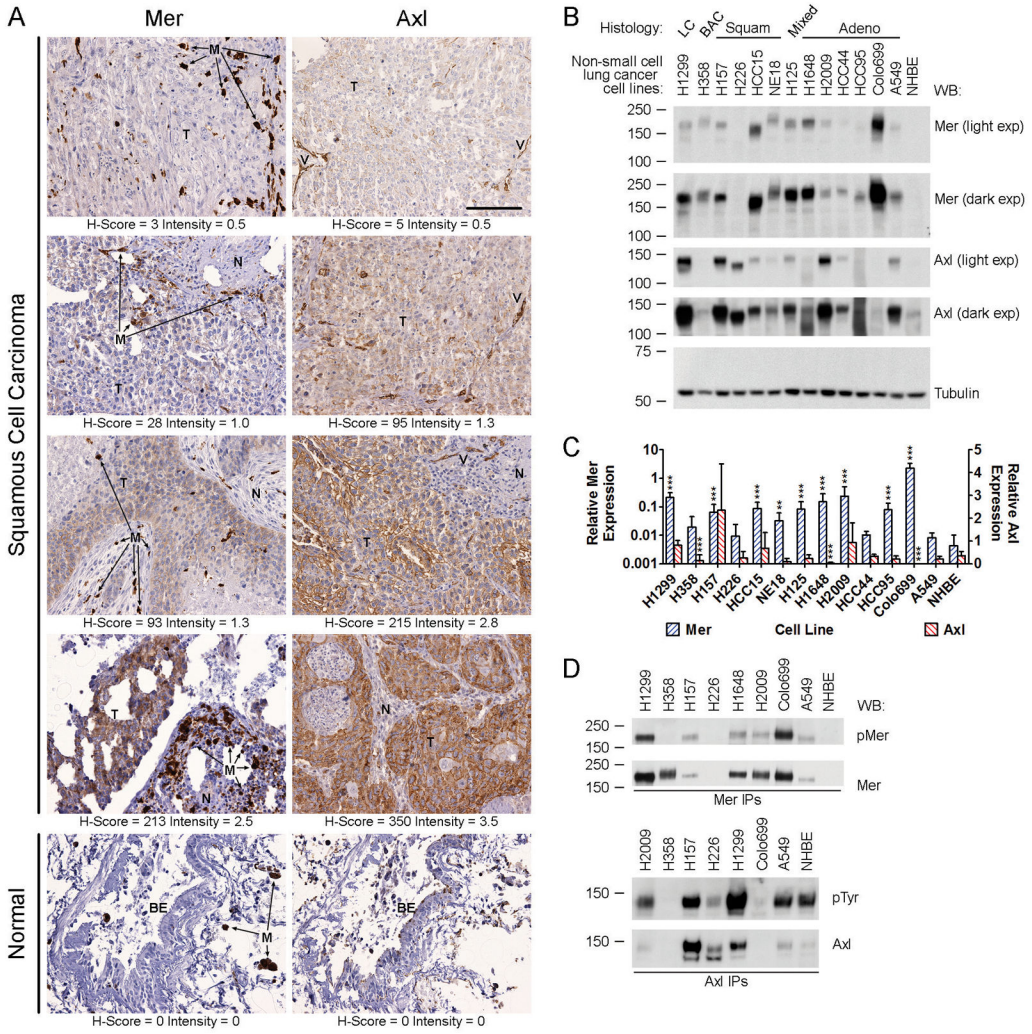

Figure 1. Mer and Axl receptor tyrosine kinases are expressed in human non-small cell lung cancer tumors and cell lines

(A) Immunohistochemical staining of Mer and Axl in sections of normal human lung and squamous cell carcinoma of human lung. Micrographs shown represent the range of staining observed in tumor cells (T). Adjacent normal tissue (N) was always negative for Mer and Axl as was bronchial epithelium (BE). Macrophages (M, arrows) were strongly positive for Mer and blood vessels (V) were strongly positive for Axl. The scale bar in the upper right panel is applicable to all micrographs and represents 100 μm. **(B)** Whole-cell lysates of the indicated cell lines were subjected to western blot (WB) analysis using the indicated antibodies. Two exposures (exp) are shown for Mer and Axl. In 13/13 NSCLC lines tested, Mer and/or Axl are overexpressed relative to levels found in normal human bronchial epithelial (NHBE) cells. Variation in the molecular weight of each receptor is likely due to cell line-specific patterns of glycosylation as the extracellular domains of Axl and Mer contain 6 and 13 glycosylation sites, respectively. Tubulin was used as a loading control. Numbers on the left indicate the location of molecular weight (kDa) markers. Blots representative of at least three independent experiments are shown. **(C)** Real-time RT-PCR

analysis of Mer and Axl mRNA transcript expression in the same collection of cell lines shown in panel B. Two-way ANOVA and Bonferroni post-tests were used to compare the mean ΔCt values derived from at least three independent measurements. The mean + SD of antilogged ΔCt values ($2^{-\Delta Ct}$) are shown. The asterisks indicate significant differences versus NHBE (*** $P < 0.001$, ** $P < 0.01$, * $P < 0.05$). **(D)** Mer and Axl were immunoprecipitated from whole-cell lysates of steady-state cultures of a subset of the NSCLC cell lines shown in A and B. Phosphorylated and total levels of Mer and Axl proteins were assessed by western blot analysis using anti-phospho-Mer (pMer, Y749/Y753/Y754, PhosphoSolutions) and anti-Mer antibodies or anti-phosphotyrosine (pTyr, Millipore, 05–1050) and anti-Axl antibodies, respectively. Blots representative of at least three independent experiments are shown.

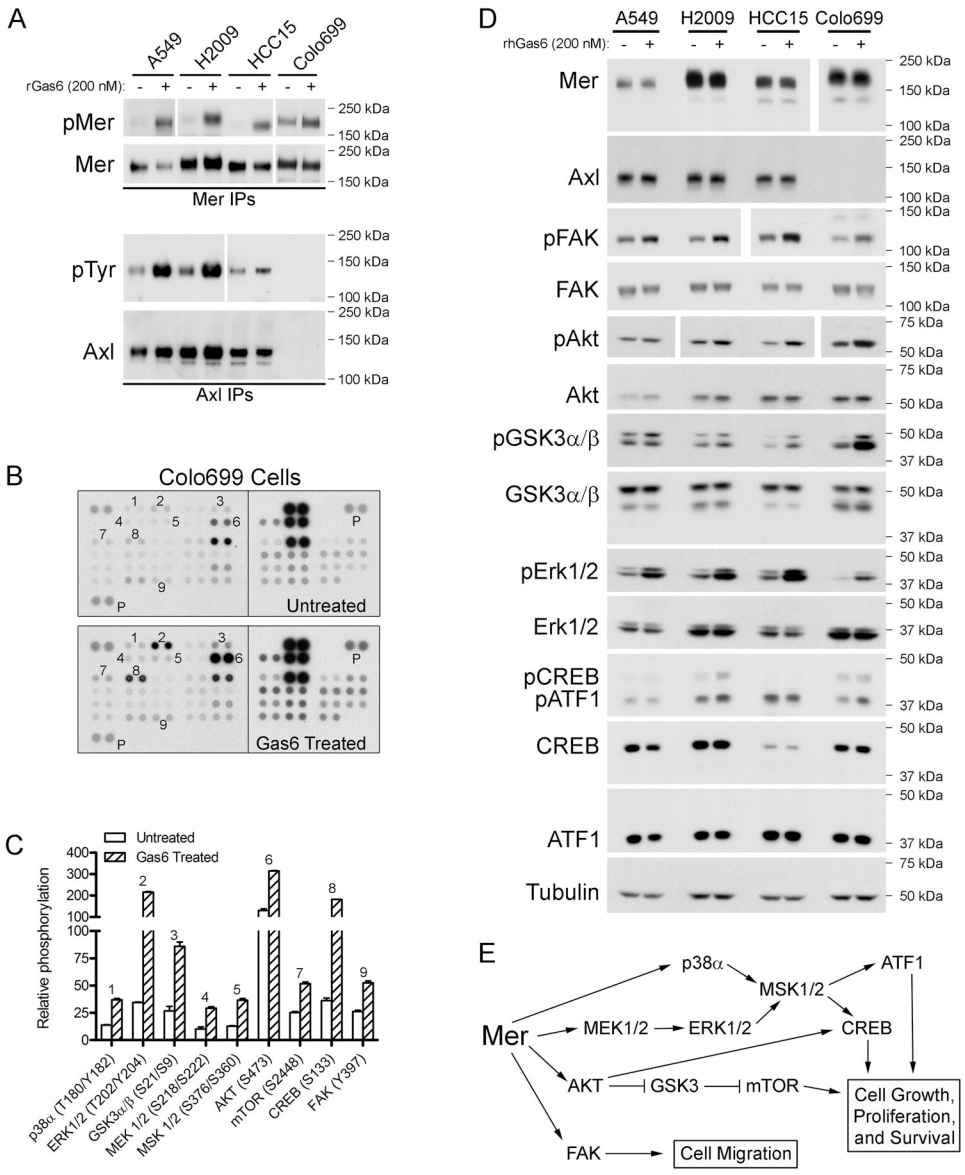

Figure 2. Ligand-dependent Mer or Axl activation stimulates MAPK, AKT, and FAK signaling pathways in NSCLC cells

Subconfluent cultures of A549, H2009, HCC15, and Colo699 NSCLC cells were incubated in serum-free medium for two hours followed by ten minute stimulation with (+) or without (−)200 nM rGas6 (human or mouse). **(A)** Mer and Axl immunoprecipitates were analyzed by western blot analysis using anti-phospho-Mer (pMer) and anti-Mer antibodies or anti-phosphotyrosine (pTyr) and anti-Axl antibodies, respectively. Due to variation in expression levels among the cell lines, longer exposure times are shown for pMer in A549 cells and for pTyr in HCC15 and Colo699 cells and shorter exposures are shown for both pMer and total Mer in Colo699 cells. Blots representative of at least three independent experiments are shown. **(B)** Diluted Colo699 lysates were incubated with human phospho-kinase array (R&D Systems, ARY003) membranes and bound phospho-proteins were detected according to kit instructions. Each membrane contains kinase specific (e.g., 1–9) and positive control

(P) antibodies spotted in duplicate. A key identifying the coordinates of each protein spotted on the array is available on the R&D Systems website (http://www.rndsystems.com/pdf/ARY003.pdf). **(C)** Relative phosphorylation of spots 1–9 was quantified by normalizing pixel density of each positive control to 100. Each bar represents the mean ± SD of duplicate spots from a single experiment. Quantification of the protein spots that did not exhibit Gas6-responsive phosphorylation is provided in Supplemental Figure 2. **(D)** Protein expression was assessed by western blot analysis of whole-cell lysates using the indicated antibodies. Numbers on the right indicate the location of molecular weight markers. Tubulin was used as a loading control. Due to variation in expression levels among the cell lines, a shorter exposure is shown for Mer in Colo699 cells and longer exposures are shown for pFKA (HCC15 and Colo699 cells) and pAkt (H2009 and HCC15 cells). Blots representative of at least three independent experiments are shown. **(E)** Flow chart of signaling modules activated downstream of ligand-dependent Mer stimulation.

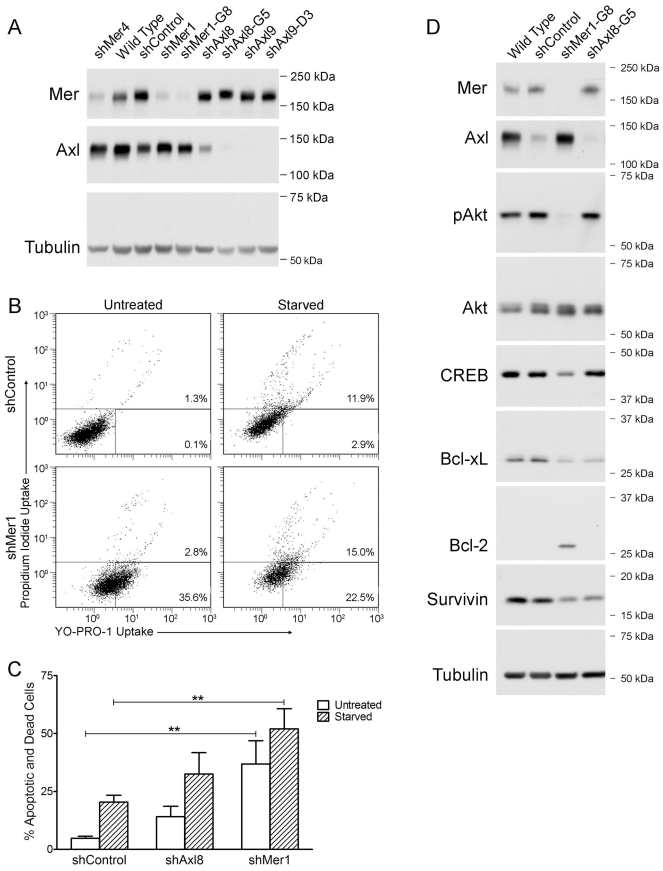

Figure 3. Mer inhibition increases apoptosis and inhibits pro-survival signaling in NSCLC cells

(A) Whole-cell lysates of the indicated A549 cell lines were subjected to western blot analysis using anti-Mer and anti-Axl antibodies. Tubulin was used as a loading control. Blots representative of at least three independent experiments are shown. **(B)** Representative scatter plots of Mer-knockdown (shMer1) and shControl A549 cells incubated in the presence (Untreated) or absence (Starved) of 10% fetal bovine serum for 1–5 hours. Apoptotic and dead cells were identified by flow cytometric analysis of cells stained with YO-PRO-1 and propidium iodide. The percentages of apoptotic (bottom right) and dead cells (top) are shown. **(C)** Cumulative data demonstrate a significant accumulation of apoptotic and dead cells when Mer expression is reduced (** $P < 0.01$ vs shControl, 2-way repeated measures ANOVA followed by Bonferroni posttests, $n = 12$). Mean values and standard errors are shown. **(D)** Wild type, shControl, shMer1-G8, and shAxl8-G5 A549 cells were cultured in serum-free medium for two hours to mimic the experimental conditions in panels B and C. Whole-cell lysates were subjected to western blotting with antibodies against the indicated proteins. Tubulin was used as a loading control. Blots representative of three independent experiments are shown.

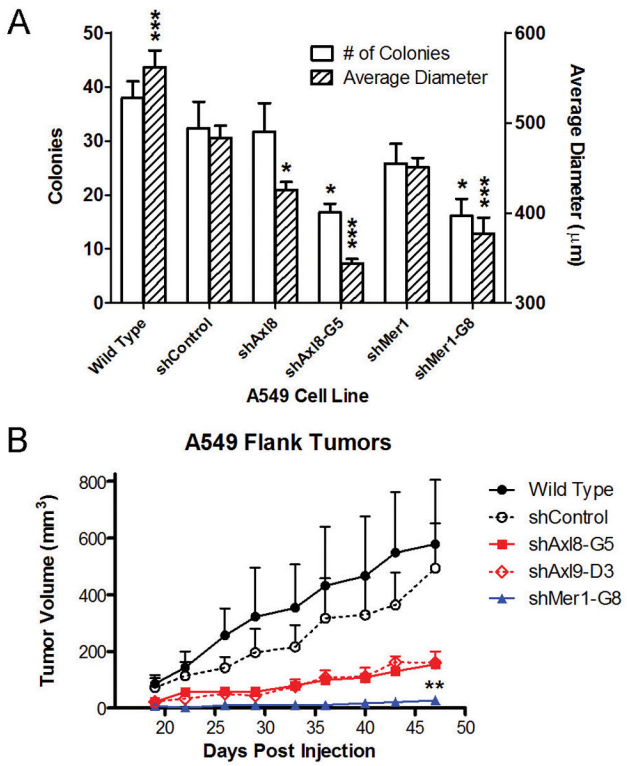

Figure 4. Inhibition of Mer or Axl reduces A549 cell clonogenic growth in vitro and prevents growth of subcutaneous xenograft tumors in vivo

(A) Clonogenic colony formation assays. Wild type, shControl, and Axl- (shAxl8, shAxl8-G5) or Mer- (shMer1, shMer1-G8) knockdown A549 cells were plated at ultra-low density and cultured for 7 days. Colony number and diameter were determined. Each bar represents the mean + SEM derived from three independent experiments performed in triplicate. One-way analysis of variance was used to compare shControl cells to all other A549 cells lines. shControl cells produced smaller colonies than wild type cells, although no difference in colony number was observed between wild type and shControl cells. * $P < 0.05$, *** $P < 0.001$, Bonferroni's Multiple Comparison Test. **(B)** Growth of A549 xenograft tumors. Mean tumor volumes and standard errors (n = 7–13 animals per group) are plotted as a function of time since cell injection. Unpaired, two-tailed, student's t-tests were used to compare mean tumor volumes versus shControl at Day 47. ** $P < 0.005$ shMer1-G8 vs. shControl. No significant difference between shControl and wild type was observed ($P = 0.7676$).

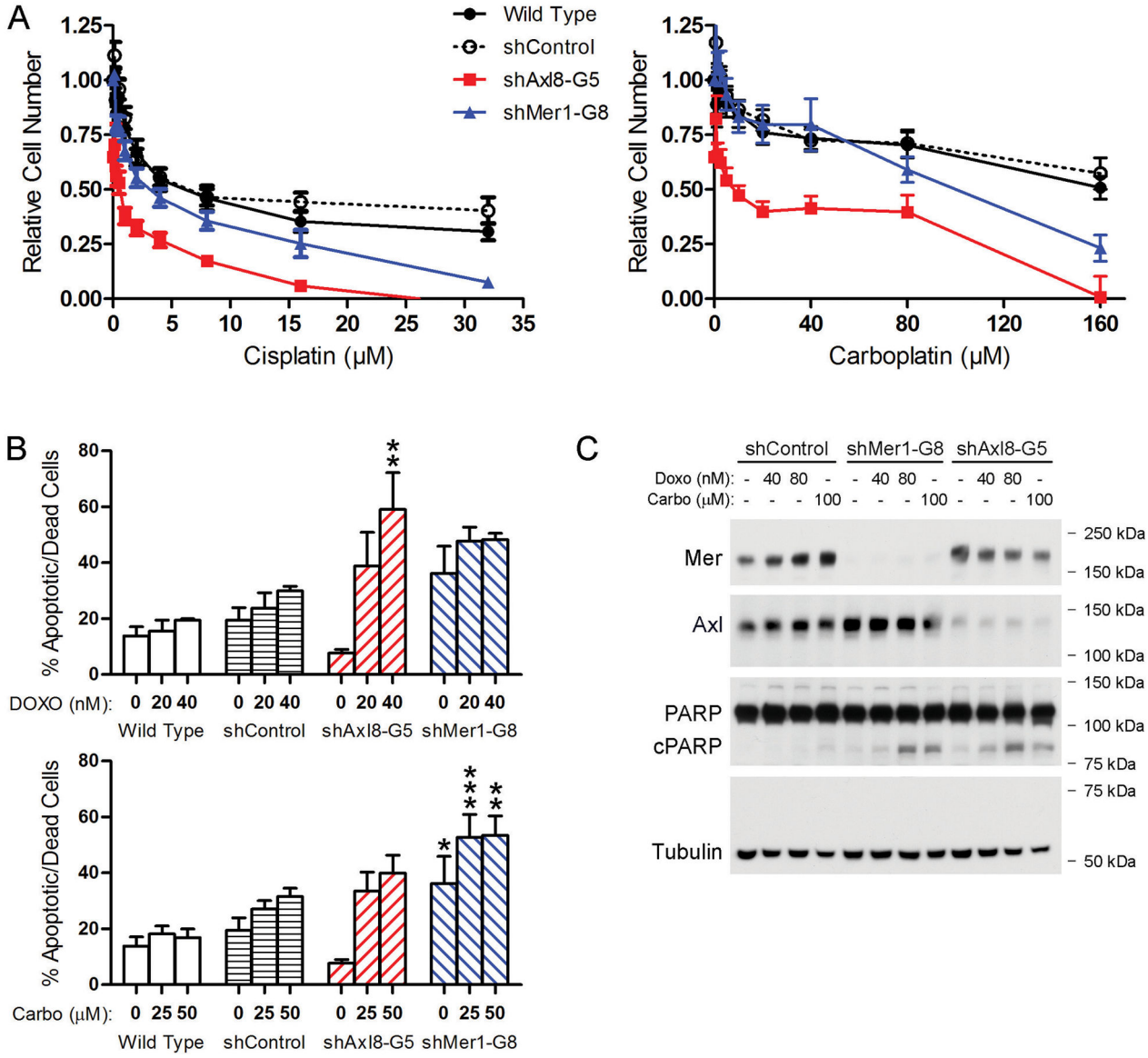

Figure 5. Mer or Axl knockdown results in enhanced chemosensitivity, increased cell death, and apoptotic pathway activation in A549 cells

Wild type, shControl, Axl-knockdown (shAxl8-G5), and Mer-knockdown (shMer1-G8) A549 cells were treated with the indicated concentrations of cisplatin, carboplatin, or doxorubicin for 24 (C) or 48 (A and B) hours. **(A)** Relative cell numbers were determined using the MTT assay. Mean values and standard errors from at least 3 independent experiments are shown. IC_{50} values are displayed in Table 2. **(B)** The percentage of apoptotic and dead cells was quantified using the YO-PRO-1/PI assay. Mean values and standard errors from at least 3 independent experiments are shown. No significant differences between wild type and shControl cells were observed. * $P < 0.05$, ** $P < 0.01$, *** $P < 0.001$, 2-way repeated measures ANOVA followed by Bonferroni posttests versus shControl. **(C)** Expression of Mer, Axl, PARP, and cleaved PARP was assessed by

immunoblotting whole-cell lysates. Tubulin was used as a loading control. Blots representative of at least three independent experiments are shown.

Table 1

Associations Between Molecular/Clinical Features and Overall Survival in 88 NSCLC Patients (univariate analysis; log-rank test). Survival time was estimated at the 25th and 50th percentiles.

			Survival at the 25th Percentile		Survival at the 50th Percentile	
Characteristic	**Patients N (%)**	**P**	**Estimate**	**95% CI**	**Estimate**	**95% CI**
Age at Diagnosis						
< 62 years	42 (48)	0.31	22	8–31	65	29–115
≥62 years	46 (52)		10	5–22	33	18–60
Gender						
Male	47 (53)	0.15	13	6–22	27	22–61
Female	41 (47)		23	7–41	71	31-NR
Stage						
I	43 (49)	0.01	23	10–52	61	45–115
II	12 (14)		17	3–71	NR	8-NR
III	23 (26)		8	2–23	24	11–36
IV	8 (9)		6	3–18	16	3–82
UNK	2 (2)					
Histology						
SCC	37 (42)	0.24	11	4–22	25	18–71
Adeno	39 (44)		18	8–31	53	28-NR
LCC	7 (8)		8	3–53	53	3-NR
BAC	5 (6)		41	22-NR	NR	22-NR
Mer H-Score						
0–4	26 (30)	0.75	11	7–23	25	12–115
5–100	56 (64)		20	6–30	52	30–112
101–200	4 (4)		7	5–43	26	5–61
201–300	1 (1)		NR	NR	NR	NR
301–400	0 (0)					
UNK	1 (1)					
Axl H-Score						
0–4	5 (6)	0.28	NR	7-NR	NR	7-NR

			Survival at the 25th Percentile		Survival at the 50th Percentile	
Characteristic	**Patients N (%)**	**P**	**Estimate**	**95% CI**	**Estimate**	**95% CI**
5–100	19 (21)		18	3–28	29	18–114
101–200	28 (32)		23	5–30	45	24–82
201–300	30 (34)		8	3–31	61	16–115
301–400	5 (6)		6	4-NR	22	4-NR
UNK	1 (1)					

SCC, squamous cell carcinoma; Adeno, adenocarcinoma; LCC, large-cell undifferentiated carcinoma; BAC, bronchioalveolar carcinoma; UNK, unknown; NR, not reached.

Table 2

IC50 values determined by non-linear regression of MTT assay data.

		A549 Human NSCLC Cell Lines				
		Wild Type	**shControl**	**shMer1-G8**	**shAxl8-G5**	**shAxl9-D3**
Cisplatin (μM)	IC50	6.48	8.56	3.00	0.51	3.40
	(95% CI)	(4.8 – 8.8)	(6.5 – 11.2)	(2.4 – 3.7)	(0.4 – 0.7)	(2.6 – 4.5)
	P<0.05	NS	-	*	*	*
Carboplatin (μM)	IC50	> 160	> 160	93.4	9.13	ND
	(95% CI)	ND	ND	(60.1 – 145)	(5.8 – 14.4)	ND
	P<0.05	ND	-	ND	ND	ND
Doxorubicin (nM)	IC50	34.9	69.2	71.2	2.1	13.0
	(95% CI)	(18.0 – 67.7)	(45.5–105.4)	(31.2 – 162)	(1.0 – 4.2)	(8.6 – 19.7)
	P<0.05	NS	-	NS	*	*
Etoposide (μM)	IC50	2.20	3.32	3.84	0.33	1.01
	(95% CI)	(1.58 – 3.05)	(2.47 – 4.46)	(2.78 – 5.30)	(0.24 – 0.46)	(0.70 – 1.46)
	P<0.05	NS	-	NS	*	*

Cumulative data from at least three independent experiments performed in triplicate were analyzed.

* Significance versus shControl is indicated by non-overlapping confidence intervals (95% CI). Significance could not be statistically evaluated for Carboplatin treated cells because an IC50 was not reached for wild type or shControl cells. Abbreviations are as follows: ND, Not determined; NS, Not significant.